ChemComm

COMMUNICATION

View Article Online
View Journal | View Issue

Cite this: *Chem. Commun.*, 2016, 52, 9291

Received 28th March 2016,
Accepted 19th June 2016

DOI: 10.1039/c6cc02618d

www.rsc.org/chemcomm

Mechanistic insights into light-driven graphene-induced peroxide decomposition: radical generation and disproportionation†

Ya-Lan Chu, Yen-An Chen, Wei-Chin Li, Jean-Ho Chu, Chun-Hu Chen* and Chao-Ming Chiang*

Interaction between adsorbed *t*-butyl peroxybenzoate and photo-excited graphene rendered trapped phenyl and *t*-butoxy radicals. Post-irradiation thermal desorption showed benzene, *t*-butanol, and isobutylene oxide as the end products. The required hydrogen atoms were obtained *via* the radical disproportionation. Graphene enabled radical species to be captured and their on-surface chemistry to be revealed.

There has been a lot of graphene hype ever since the discovery of this two-dimensional wonder material, stimulating immense interest across multiple disciplines.[1,2] Chemists are not immune to this fascination.[3] Chemical functionalization is a remedy to the zero bandgap and solubility problems of graphene.[4–7] However, the chemical inertness, due to its fully conjugated sp^2 carbon network and lack of curvature, presents a formidable challenge to modify graphene with covalently bonded organic groups. A free radical addition approach is one of the solutions to address this issue. Brus and co-workers pioneered the photochemical treatment using dibenzoyl peroxide (DBP) as a phenyl radical precursor.[8] A lower electrical conductivity as compared to the starting graphene was obtained, indicating the attachment of sp^3 moieties onto the basal plane of graphene, but direct evidence for the phenyl radical remained elusive. Photoinduced methylation of graphene was achieved by Liu *et al.* using supported graphene films immersed in a di-*t*-butyl peroxide (DTBP) solution and irradiated using a mercury lamp.[9,10] Direct photolysis was suggested as the source of methyl radicals but without mechanistic details. Because all these feats were accomplished by wet-chemical routes, radical detection might be difficult at the graphene–liquid interface. An equivalent investigation under ultrahigh vacuum (UHV) conditions, using the *in situ* tools available within the realm of surface science, would circumvent the obstacle and unveil the various light triggered radical–radical and/or radical–graphene interactions.

Department of Chemistry, National Sun Yat-Sen University, Kaohsiung, 80424, Taiwan. E-mail: chunhu.chen@mail.nsysu.edu.tw, cmc@mail.nsysu.edu.tw

† Electronic supplementary information (ESI) available: Experimental details and spectroscopic characterization. See DOI: 10.1039/c6cc02618d

Here *t*-butyl peroxybenzoate (TBPB), a composite of DBP and DTBP with the –O–O– moiety flanked unsymmetrically by a benzoyl group (PhCO–) and a *t*-butyl group ($(CH_3)_3C$–), was chosen deliberately as the radical precursor because homolytic O–O bond scission would first produce two oxygen-centered radicals; however, the benzoyloxy fragment ($PhCOO^{\bullet}$) may lose CO_2 to give the phenyl radical while the *t*-butoxy unit ($(CH_3)_3CO^{\bullet}$) can convert to the methyl radical by releasing 1 equivalent of acetone.[9] It is curious to know whether phenylation or methylation of graphene can be steered by adopting such a hybrid. Metal-supported single layer graphene (SLG) was selected over exfoliated graphene flakes considering its suitability for the surface infrared characterization. Because SLG exhibited higher reactivity than its double- and multi-layer counterparts,[8,9] it should be more prone to functionalization. SLG was prepared by chemical vapour deposition (CVD) in which hydrogen-pretreated Cu foils were exposed to a mixture of regulated hydrogen and methane flows in a quartz tube furnace at 1000 °C (the details are provided in the ESI†). The single-layer and defect-free nature was confirmed by confocal Raman spectroscopy (Fig. S1, ESI†). The copper-supported graphene sample (SLG/Cu) was then transferred into a UHV apparatus capable of performing temperature programmed desorption (TPD) and reflection–absorption infrared spectroscopy (RAIRS) measurements (see the experimental details in the ESI†). Multiple-ion TPD, a technique for monitoring the interaction between an adsorbate and a substrate, exhibits in Fig. 1(a) that after dosing SLG/Cu with 0.1 L (a unit of exposure, 1 L = 10^{-6} Torr s) TBPB at 200 K desorption of intact peroxide molecules led to two separate features, characterized by a set of concurrent *m*/*z* 194 (parent ion), 105 ($PhCO^+$, the base peak for the TBPB[11]), 77 (Ph^+), 59 ($(CH_3)_2COH^+$), 51 ($C_4H_3^+$), 43 ($(CH_3)CO^+$), 41 ($C_3H_5^+$) and 31 (CH_3O^+) signals. Sequential dosing experiments from 0.02 to 2.0 L (see Fig. 1(b)) revealed that the 277 K high-temperature state which we assign to desorption from defects along domain boundaries of the CVD grown graphene[12] (confirmed by the small Raman D band at 1340 cm^{-1}) was populated and saturated first. As the exposure is increased to 1 L twin peaks can be observed at 224 K and 231 K and are attributed to desorption from the

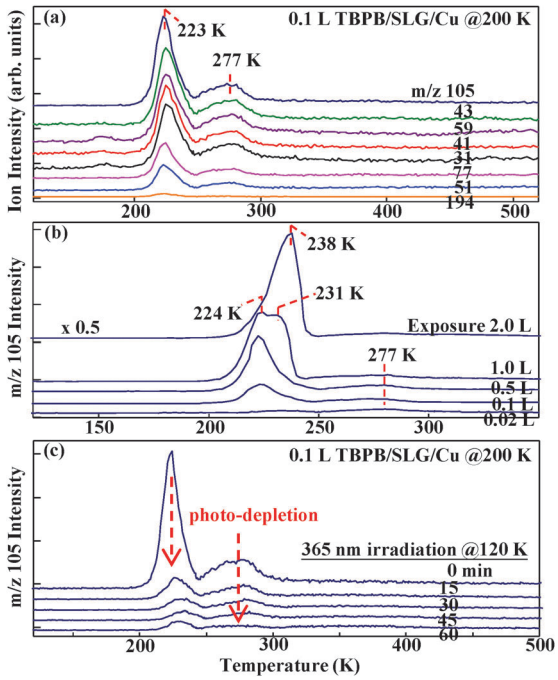

Fig. 1 (a) Multiplex TPD spectra measured after exposing 0.1 L TBPB to SLG/Cu at 200 K. (b) Trend of *m*/*z* 105 (the most abundant fragment for TBPB) ion signals as a function of TBPB exposure. The 0.1 L exposure would correspond to a submonolayer coverage. (c) Trend of *m*/*z* 105 signals as a function of UV irradiation time.

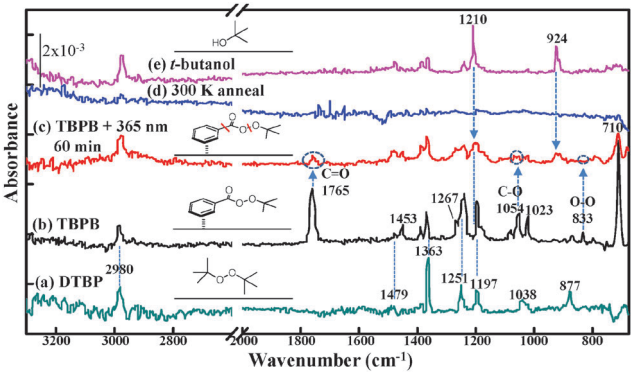

Fig. 2 RAIR spectra of (a) DTBP dosed on SLG/Cu at 120 K, (b) 0.1 L TBPB dosed on SLG/Cu at 200 K, (c) sample (b) after 60 minutes of UV irradiation, (d) sample (c) following vacuum annealing to 300 K, and (e) *t*-butanol dosed on SLG/Cu at 120 K. The drawings serve to assist in vibration mode assignments; no molecular-level structural details are implied.

monolayer and thick films on the domain interior of graphene, respectively. The fact that the monolayer desorption temperature is lower than the multilayer indicates that the adsorbate–surface interactions are slightly weaker than the adsorbate–adsorbate interactions (TBPB is a low vapour pressure liquid, 0.2 Torr at 75 °C). With increasing exposure these two low-temperature peaks merge into one and continue to grow. RAIR spectra of adsorbed TBPB without light irradiation were taken at various annealing temperatures (Fig. S2, ESI†). As illustrated in Fig. S2(b) and (c) (ESI†), heating above the molecular desorption temperature rendered the spectra to become featureless. The lack of spectral changes associated with molecular transformation suggests that TBPB molecules simply adsorb and desorb reversibly. We were unable to thermally activate them on graphene.

Intriguingly, following the adsorption of TBPB at 200 K peroxide species were found to be depleted from the graphene by UV irradiation at 120 K using 365 nm high-power LEDs (the details are provided in the ESI†), as evidenced by a series of post-irradiation temperature programmed desorption (PITPD) traces displayed in Fig. 1(c) where the diminishing trend of *m*/*z* 105 intensities with prolonged UV exposure time is highlighted. Two obvious channels can account for the loss of TBPB: photodesorption and photodissociation. An attempt to detect the desorbing species in the presence of light was proven to be unsuccessful because the sensitivity of the quadrupole mass spectrometer (QMS) was attenuated while the sample was in the irradiation position (QMS head was retracted and located 45° from the incident light to avoid shadowing the surface). However, photodissociation of TBPB can be confirmed by comparing the RAIR spectra measured prior and subsequent to the UV exposure. Following the 0.1 L TBPB adsorption at 200 K, key vibration modes are noted at 1765 cm^{-1} (typical C=O stretch for the ester carbonyl),[13] 833 cm^{-1} (O–O single-bond stretch for peroxide),[14] 710 cm^{-1} (ring C–H out-of-plane bend) in Fig. 2(b). According to the surface dipole selection rule, the domination of the out-of-plane mode suggests that at such a low coverage the phenyl ring of TBPB lies flat on the surface, attributable to the π–π stacking between phenyl and graphene. The strong carbonyl signal indicates that the C=O bond is perpendicular to the surface and extends into vacuum. The assignments for the rest of the IR bands are facilitated by first recognizing the similarities between adsorbed TBPB and DTBP whose IR bands are more well-defined[15] and featured by 2980 (CH_3 stretch), 1479 (CH_3 asymmetric deformation), 1363 (CH_3 symmetric deformation), 1251 (skeletal C–C stretch), 1197 ($(CH_3)_3C$–O stretch), 1038 (CH_3 rock), and 877 (O–O stretch) cm^{-1} absorptions illustrated in Fig. 2(a). By eliminating the peaks belonging to *t*-butoxy, vibrations associated with the benzoyloxy group, including 1453 (ring stretch), 1267 (ring C–H in-plane bend), 1054 (ester C–O stretch), and 1023 cm^{-1} (ring C–H in-plane bend), become evident in Fig. 2(b). As shown in Fig. 2(c), signature bands corresponding to the peroxy (833 cm^{-1}) and the ester (1765 and 1054 cm^{-1}) functionalities clearly diminish or vanish in the RAIR spectrum taken after 60 minutes of UV irradiation, suggesting the rupture of the weak O–O bond instantaneously followed by Ph–C bond scission (decarboxylation) within TBPB molecules.[16,17] The remaining modes, such as CH_3 stretch, CH_3 deformations, $(CH_3)_3C$–O stretch, and ring C–H bends, might represent the photogenerated *t*-butoxy and phenyl radical species ($PhCOO-OC(CH_3)_3 \rightarrow (CH_3)_3CO^{\bullet} + Ph-COO^{\bullet}$; $Ph-COO^{\bullet} \rightarrow Ph^{\bullet} + CO_2$) co-trapped on the copper-supported graphene at 120 K. Control experiments were performed by replacing SLG/Cu with a bare Cu(111) as the substrate. Completely different chemistry was found. It turns out that TBPB was subjected to thermolysis even at 200 K and the O–O bond was disrupted, resulting in IR spectra featured by a strong absorption band at 1410 cm^{-1} which is assigned to the symmetric carboxylate

O═C–O stretching mode for chemisorbed benzoate species in an upright conformation (Fig. S3, ESI†).[18,19] Conversion to the benzoate–Cu was fully accomplished at 250 K and the species can persist up to 500 K. In sharp contrast, the IR features faded out entirely (see Fig. 2(d)) through 300 K vacuum annealing on SLG/Cu; therefore covalently bonded species were excluded. Namely, neither phenylation nor methylation was achieved. In the successful wet-chemical functionalization,[8–10] active species were generated under ambient conditions, whereas radicals in our experiments were created at the cryogenic temperature at which the radical reactivity would be attenuated and incapable of challenging graphene. In fact, a clean graphene surface could always be reproduced by annealing the sample to 700 K under vacuum. The integrity of the graphene layer was not affected by repeated dose and thermal desorption cycles. A closer inspection of Fig. 2(c) also shows new features emerging at 924 and 1210 cm^{-1} which match remarkably well with the IR frequencies for adsorbed *t*-butanol (see Fig. 2(e)).

Inspired by this observation, extensive mass search was conducted in the PITPD experiments to elucidate the fate of radicals produced photochemically on graphene. First, the absence of methane and acetone suggests that the *t*-butoxy radical did not proceed to form the methyl radical. By checking the differences in the TPD results with and without UV irradiation (see middle and top panels in Fig. 3), benzene, instead of benzoic acid (PhCOOH), was identified (see Fig. 3(a)). Thus the decarboxylation step is further consolidated. In addition, *t*-butanol ($(CH_3)_3CO^{\bullet}$ + $H^{\bullet}$ → $(CH_3)_3COH$) was also recognized in Fig. 3(b). Benzene and *t*-butanol can both be ratified by the same relative abundance of the major mass fragments in the TPD profiles taken after exposing vapours of the pure compounds to SLG/Cu (see bottom panels in Fig. 3(a) and (b)). The agreement in desorption maxima together with their low-temperature (160 K for benzene and 175 K for *t*-butanol) implies that the photochemical generation and termination of radicals are facile and require little activation energies.

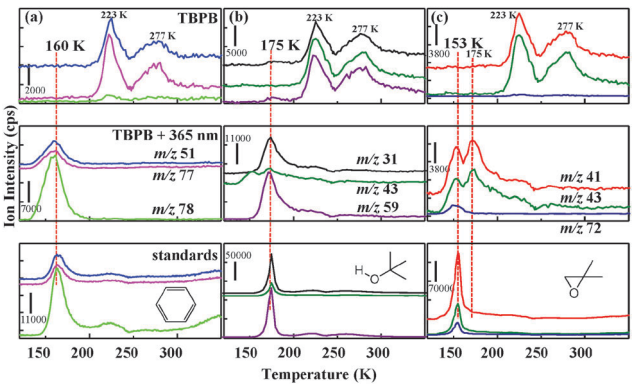

Fig. 3 (a) Diagnostic multiple-ion TPD spectra for identifying benzene at *m/z* 51, 77, and 78 (parent ion) measured after 0.1 L TBPB adsorption on SLG/Cu at 200 K (top), after 0.1 L TBPB adsorption on SLG/Cu at 200 K, followed by UV irradiation at 120 K for 60 min (middle), and after exposing pure benzene directly to SLG/Cu (bottom), (b) the same type of experiments except for identifying *t*-butanol at *m/z* 31, 43, and 59 (base peak), and (c) the same type of experiments for identifying isobutylene oxide at *m/z* 41, 43, and 72 (parent ion).

The last step, desorption of the end-products, is presumably rate-limiting. Because the initial adsorption of the reactant was carried out at 200 K (higher than the product desorption temperatures), a consequence due to the extraneous impurities admitted into the UHV chamber should be ruled out.

To explain the origin of the hydrogen atoms, radical disproportionation[20] reactions must be invoked under solvent-free conditions. In typical radical disproportionation one radical plays the role of an acceptor while the other acts as a hydrogen donor. Each *t*-butoxy radical has nine methyl hydrogens to donate; therefore, cross disproportionation of a $^{\bullet}OC(CH_3)_3$/$^{\bullet}$Ph pair should give rise to two stable products: a new $C(sp^2)$–H bond is constructed to make benzene at the expense of breaking a methyl C–H bond. In the meantime, the transient $^{\bullet}OC(CH_3)_2CH_2^{\bullet}$ species may readily build a head-to-tail C–O linkage to yield a cyclic ether (isobutylene oxide), or it undergoes further rearrangement to afford a 2-butanone (methyl ethyl ketone) isomer. This rationale gains strong support from the desorbing species at 153 K (see the middle panel in Fig. 3(c)) that was otherwise absent in the dark (top panel) following TBPB adsorption and UV irradiation. The *m/z* signals at this temperature decrease in the order of 41 ($C_3H_5^+$) > 43 ($C_3H_7^+$) > 72 ($C_4H_8O^+$, parent ion), and the trend is mirrored fairly well with the relative intensity pattern obtained from pure isobutylene oxide (Fig. 3(c), bottom panel) rather than 2-butanone whose most abundant fragment ion would be *m/z* 43 (data not provided). The termination at the cyclic ether is novel but not unprecedented. The same species was once spectroscopically identified for the thermal decomposition of DTBP in pellets of KBr.[21] It is noteworthy that the product, *t*-butanol, contributes to the additional *m/z* 41 and 43 fragments shown at 175 K. In fact, it is logical to expect *t*-butoxy radicals to engage in self-disproportionation, thereby creating *t*-butanol and isobutylene oxide as well. One of the driving forces for radical disproportionation reactions is provided by the high exothermicity resulting from the newly formed $C(sp^2)$–H, O–H, and C–O bonds. Although the paths available to a pair of radicals certainly include recombination (coupling), additional mass fragments, pertinent to ethane (CH_3–CH_3), biphenyl (Ph–Ph), DTBP ($(CH_3)_3CO$–$OC(CH_3)_3$), benzoyl peroxide (PhCOO–OOCPh), toluene (Ph–CH_3), and *t*-butoxy benzene ($(CH_3)_3CO$–Ph) were surveyed but not found in PITPD measurements. We interpret that the preference for disproportionation over recombination rests on the large number of transferable hydrogens to donate on the *t*-butoxy radicals and the entropy effect. On the other hand, the more electronegative oxygen facilitates an alkoxy radical itself as an acceptor to abstract hydrogen, so the dual role of the *t*-butoxy radical can account for the diversity of the final products in this case.

Graphene played a crucial part in the discovery. TBPB does not absorb the 365 nm photons (see Fig. S4 in the ESI† for the UV spectrum) but graphene does.[22] As Brus and coworkers have suggested,[8] photoexcited graphene (GR*) can serve as a photosensitizer responsible for transferring one electron into the LUMO of TBPB. In concomitance with the relocation of another electron from the TBPB HOMO to graphene, such a two-way electron-exchange mechanism results in a net energy transfer (ET) process and the formation of ground-state graphene (GR)

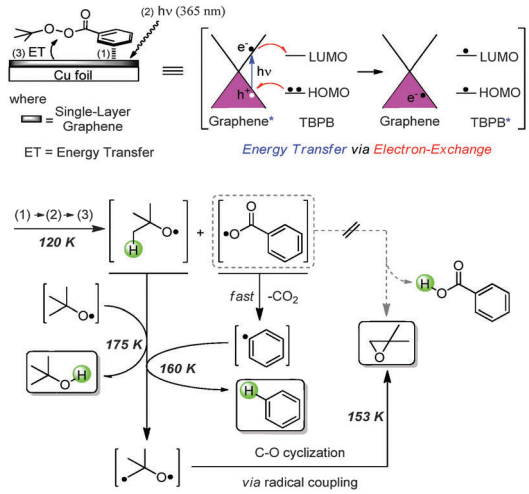

Fig. 4 Proposed reaction mechanism.

and excited-state TBPB (TBPB*) that cannot be reached by direct photon excitation. TBPB* is expected to decompose *via* homolytic cleavage of the O–O bond to produce $(CH_3)_3CO^{\bullet}$ and Ph–$COO^{\bullet}$. The π–π interactions, indicated by IR, brought TBPB and graphene in close proximity and the intimate interfacial contact facilitated the ET pathway. Graphene also behaved like a solid matrix exploited in the matrix isolation technique which enables reactive chemical species to be isolated and studied spectroscopically. The chemical inertness of the matrix material prevents loss of reactive species. Here graphene was proven to be unreactive towards phenyl and *t*-butoxy radicals generated from adsorbed TBPB by UV exposure. These photogenerated radicals were intercepted at the cryogenic temperature on graphene, then became mobile and started to explore many configurations until finding the right partners (another radical to be exact) in two dimensions (2D) during the annealing stage of matrix warm-up.

In conclusion, our study represents the first example of using UV-LEDs as the photon source to initiate decomposition of an unsymmetrical peroxide composed of *t*-butoxy and benzoyloxy groups, bound to the metal-supported graphene under UHV conditions. Direct surface IR detection infers that both O–O and Ph–C bonds were cleaved upon irradiation, suggesting that *t*-butoxy and phenyl radicals were *in situ* generated and trapped on graphene. Desorption of *t*-butanol and benzene observed in PITPD resonates with the formation of the proposed radicals. Our proposed mechanism is depicted in Fig. 4. Although no evidence supports covalent interactions between the radicals and the graphene carbon, graphene's resistance to free radical attack turns out to be an asset. Graphene acts like a 2D host matrix on which identities and different types of interactions of the guest radicals can be established. Disproportionation serves admirably to explain the origin of the hydrogens for the end-products, and the donor–acceptor roles in the abstraction mechanism are well resolved. These findings demonstrate graphene as a unique mechanistic tool to probe free radical reaction pathways that are not observable under ambient conditions. In light of this prototypical study, further experiments on unstable species such as nitrene and carbene are being undertaken to explore the generalization of the concepts. Given the photosensitizer role of graphene, it is also desirable to use graphene-based semiconductor composites as a platform for photocatalysis.

We are grateful for the financial support from the Ministry of Science and Technology of ROC under Contract No. MOST 103-2113-M-110-005 and 104-2113-M-110-007.

Notes and references

1 A. K. Geim and K. S. Novoselov, *Nat. Mater.*, 2007, **6**, 183–191.
2 X. Zhang, B. R. S. Rajaraman, H. Liu and S. Ramakrishna, *RSC Adv.*, 2014, **4**, 28987–29011.
3 L. Liao, H. Peng and Z. Liu, *J. Am. Chem. Soc.*, 2014, **136**, 12194–12200.
4 V. Georgakilas, M. Otyepka, A. B. Bourlinos, V. Chandra, N. Kim, K. C. Kemp, P. Hobza, R. Zboril and K. S. Kim, *Chem. Rev.*, 2012, **112**, 6156–6214.
5 L. Yan, Y. B. Zheng, F. Zhao, S. Li, X. Gao, B. Xu, P. S. Weiss and Y. Zhao, *Chem. Soc. Rev.*, 2012, **41**, 97–114.
6 C. K. Chua and M. Pumera, *Chem. Soc. Rev.*, 2013, **42**, 3222–3233.
7 J. Park and M. Yan, *Acc. Chem. Res.*, 2013, **46**, 181–189.
8 H. Liu, S. Ryu, Z. Chen, M. L. Steigerwald, C. Nuckolls and L. E. Brus, *J. Am. Chem. Soc.*, 2009, **131**, 17099–17101.
9 L. Liao, Z. Song, Y. Zhou, H. Wang, Q. Xie, H. Peng and Z. Liu, *Small*, 2013, **9**, 1348–1352.
10 L. Zhang, L. Zhou, M. Yang, Z. Liu, Q. Xie, H. Peng and Z. Liu, *Small*, 2013, **9**, 1134–1143.
11 I. S. Krull and A. Mandelbaum, *Org. Mass Spectrom.*, 1976, **11**, 504–510.
12 P. Y. Huang, C. S. Ruiz-Vargas, A. M. van der Zande, W. S. Whitney, M. P. Levendorf, J. W. Kevek, S. Garg, J. S. Alden, C. J. Hustedt, Y. Zhu, J. Park, P. I. McEuen and D. A. Muller, *Nature*, 2011, **469**, 389–393.
13 W. H. T. Davison, *J. Chem. Soc.*, 1951, 2456–2461.
14 K. Nakamoto, *Infrared and Raman Spectra of Inorganic and Coordination Compounds*, Wiley, New York, 1997, 5th edn, p. 155.
15 D. C. McKean, J. L. Duncan and R. K. M. Hay, *Spectrochim. Acta*, 1967, **23A**, 605–609.
16 B. Abel, J. Assmann, P. Botschwina, M. Buback, M. Kling, R. Oswald, S. Schmatz, J. Schroeder and T. Witte, *J. Phys. Chem. A*, 2003, **107**, 5157–5167.
17 M. Buback, M. Kling, S. Schmatz and J. Schroeder, *Phys. Chem. Chem. Phys.*, 2004, **6**, 5441–5455.
18 C. C. Perry, S. Haq, B. G. Frederick and N. V. Richardson, *Surf. Sci.*, 1998, **409**, 512–520.
19 J. Lee, D. B. Dougherty and J. T. Yates, Jr., *J. Am. Chem. Soc.*, 2006, **128**, 6008–6009.
20 M. J. Gibian and R. C. Corley, *Chem. Rev.*, 1973, **73**, 441–464.
21 H. A. Bent and B. Crawford, Jr., *J. Am. Chem. Soc.*, 1957, **79**, 1793–1797.
22 E.-Y. Choi, T. H. Han, J. Hong, J. E. Kim, S. H. Lee, H. W. Kim and S. O. Kim, *J. Mater. Chem.*, 2010, **20**, 1907–1912.

